Published in final edited form as:
Bioconjug Chem. 2009 February ; 20(2): 274–282. doi:10.1021/bc8003638.

Compared to Purpurinimides, the Pyropheophorbide Containing an Iodobenzyl Group showed Enhanced PDT Efficacy and Tumor Imaging (^{124}I-PET) Ability

Suresh K. Pandey[1], **Munawwar Sajjad**[3,*], **Yihui Chen**[1], **Anupam Pandey**[1,¶], **Joseph R. Missert**[1], **Carrie Batt**[1], **Rutao Yao**[3], **Hani A. Nabi**[3], **Allan R. Oseroff**[2], and **Ravindra K. Pandey**[1,*]

1*PDT Center, Cell Stress Biology, Roswell Park Cancer Institute, Buffalo, NY 14263*

2*Department of Dermatology, Roswell Park Cancer Institute, Buffalo, NY 14263*

3*Department of Nuclear Medicine, State University of New York, Buffalo, NY 14214*

Abstract

Two positional isomers of purpurinimide; 3-[1'-(3-iodobenzyloxyethyl)] purpurin-18-N-hexylimide methyl ester **4** in which the iodobenzyl group is present at the top half of the molecule (position-3) and a 3-(1'-hexyloxyethy)purpurin-18-N-(3-iodo-benzylimide)] methyl ester **5**, where the iodobenzyl group is introduced at the bottom half (N-substitued cyclicimide) of the molecule were derived from chlorophyll-a. The tumor uptake and phototherapeutic abilities of these isomers were compared with the pyropheophorbide analog **1** (lead compound). These compounds were then converted into the corresponding ^{124}I- labeled PET imaging agents with specific activity >1Ci/μmole. Among the positional isomers **4** and **5**, purpurinimide **5** showed enhanced imaging and therapeutic potential. However, the lead compound **1** derived from pyropheophorbide-a exhibited the best PET imaging and PDT efficacy. For investigating the overall lipophilicity of the molecule, the 3-O-hexyl ether group presnt at position-3 of purpurinimide **5** was replaced with a methyl ether substituent and the resulting product **10** showed improved tumor uptake, but due to its significantly higher uptake in liver, spleen and other organs, a poor tumor contrast in whole-body tumor imaging was observed.

Keywords

Photosensitizer; Photodynamic Therapy; Positron Emisssion Tomography; ^{124}I-nuclide

Introduction

Positron emission tomography (PET) has wide appeal for research at the drug development stage as it allows studying the drug distribution non-invasively (1). Dedicated animal PET systems whose resolution could reach near 1 mm have intensified this field by enabling drug studies with murine disease models. In recent years, ^{18}F-fluorodeoxyglucose (^{18}F-FDG) has been the primary PET tracer. It is being used in the evaluation of several neoplasms, both before

*Address for correspondence Ravindra K. Pandey, Ph.D., PDT Center, Cell Stress Biology, Roswell Park Cancer Institute, Buffalo, NY 14263, Phone: 716-845-3203; Fax: 716-845-8920, E-mail: ravindra.pandey@roswellpark.org, Munawwar Sajjad, Ph.D., Department of Nuclear Medicine, State University of New York, Buffalo, NY 14214, Phone: 716-838-5889 ext. 118; Fax: 716-838-4918, E-mail: msajjad@buffalo.edu.
¶Undergraduate summer student (2007), SUNY, Geneseo, NY

and after therapy, as well as the planning of the radiotherapy in various cancers. Its use in the assessment of cancer after therapy, including restaging tumors and monitoring tumor response has been of particular interest for oncologists. However, ^{18}F-FDG suffers from pitfalls in cases such as where tumors are not metabolically active enough. Additionally, a short half-life of ^{18}F-isotope (110 min) limits its use in studies involving antibodies and photosensitizers (PS) related to porphyrins for the use in photodynamic therapy (PDT), which take considerably longer time to accumulate in tumor in high concentrations (2). In this respect, ^{124}I- is a better choice due to its half-life of 4.2 days (3,4). The labeling technique for ^{124}I-nuclide is now well established and this approach is continuously being followed to label a variety of biologically active molecules (5-12). In the past few years various porphyrin-based photosensitizers have been labeled/chelated with ^{111}In, ^{113}Sn and ^{99m}Tc radionuclide for the purpose of scintigraphy (SPECT) (13-21). The metallation of porphyrin core however alters the physico-chemical characteristic of the molecule. The clinically effective PS have also been labeled with ^{131}I, ^{14}C and ^{3}H mainly for the purpose to understand their pharmacokinetic and phamacodynamic characteristics (22-26). There are a few reports in the field of PDT where various F-18 based radiotracers such as ^{18}F-FDG (27-29), ^{18}F-FHBG{9-(4-^{18}F-fluoro-3-hydroxymethyl-butyl)guanine}(30), ^{18}F-FLT (3'-deoxy-3'-18F-fluorothymidine) (31) and ^{99m}Tc-Annexin V (32) have been used to monitor cellular events during and post PDT *in vivo*.

One of the main reasons for using the porphyrin-based compounds in phototherapy is due to their ability to retain in tumor (33-35). The tumor localizing ability of certain porphyrins has also been explored in developing "Multifunctional Agents", where these compounds were used as vehicles to deliver the desired imaging moieties (fluorescence, MRI, PET) to tumors (36-41).

For quite some time one of the objectives of our laboratory has been to develop photosensitizers with long absorption wavelength > 700. Irradiation of tumors with light in this range should allow deeper tissue penetration, which may help in treating the large and deeply seated tumors. To achieve our goal, we modified the *in vivo* unstable purpurin-18 and bacteriopurpurin systems, and synthesized a series of tumor-avid N- and O-alkyl- or the corresponding trifluoromethylbenzyl substituted purpurinimides (700 nm) and bacteriopurpurinimides (800 nm) with variable lipophilicity (42-43). Some of the synthetic analogs showed promising *in vivo* activity. Interestingly, among the compounds with similar lipophilicity, the position of the substituents at various peripheral position of the tetrapyrrolic system showed a significant difference in long-term tumor response.

Herein, we report the synthesis of the iodobenzyl substituted purpurinimides **4** and **5** (positional isomers) and their significant difference in PDT efficacy. The comparative biodistribution properties of the corresponding ^{124}I- analogs as well as their tumor imaging (PET) abilities are also discussed.

EXPERIMENTAL PROCEEDURES

Chemistry

All chemicals were of reagent grade and used as such. Solvents were dried using standard methods. Reactions were carried out under nitrogen atmosphere and were monitored by precoated (0.20mm) silica TLC plastic sheet (20 × 20 cm) strips (POLYGRAM® SIL N-HR) and/or UV-visible spectroscopy. Silica gel 60 (70-230 mesh, Merck) was used for column chromatography. Melting points were determined on Fisher - Johns melting point apparatus. UV-visible spectra were recorded on a Varian (Cary -50 Bio) spectrophotometer. ^{1}H-NMR spectra were recorded on Brucker AMX 400 MHz NMR spectrometer at 303 K. Proton chemical shifts (δ) are reported in parts per million (ppm) relative to $CDCl_3$ (7.26 ppm),

pyridine-d_5 (7.22 ppm, most downfield) or TMS (0.00 ppm). Coupling constants (J) are reported in Hertz (Hz) and s, d, t, q, p, m and br refer to singlet, doublet, triplet, quartet, pentet, multiplet and broad respectively. HRMS data were obtained from Mass Spectroscopy facility of Michigan State University. Analytical HPLC was used to assess the purity of compounds. Waters (Milford, MA) system including waters 600 Controller, Delta 600 pump and 996 Photodiode Array Detector was used. Reverse phase, Symmetry® C18, 5μm, 4.6 × 150 mm column (Waters, Made in Ireland) was used under an isocratic setting of MeOH/H_2O for final compounds (**1, 4, 5**, and the corresponding trimethyl stannyl analogs). Solvent flow rate was kept constant at 1.00 mL/min and detector was set at 254, 410, 535 & 660 nm (for pyropheophorbides −*a* **1**, and its trimethyl stannyl derivative) and 254, 415, 545 & 700 nm (for purpurininimides **4, 5**, and their trimethyl stannyl derivatives). All final products were found to be >95 % pure and their retention time is reported in characterization section. Reactions were first carried out for non-radioactive iodine, and analyzed in above HPLC system. However in case of final I-124 radiolabeling HPLC data obtained from above system were transferred to another system comprised of a Chrom Tech Iso-2000 pump, Hitachi L-4000 UV detector and a radiation detector. These detectors are connected to a computer with HP Chemstation software via HP 35900E interface. A Bioscan system 200 imaging scanner was used for thin layer chromatography of the radiolabeled compounds.

Synthesis of 3-{1'- (3-iodobenzyloxy)ethyl}pyropheophorbide-*a* methyl ester (1)

It was synthesized by following our previously reported procedure.[40] Yield: 77%. MP = 112-114°C; Analytical RP HPLC (95/5: MeOH/H_2O): t_R = 20.97min, >96%. UV-vis (MeOH): 662 (4.75×10^4), 536 (1.08×10^4), 505 (1.18×10^4), 410 (1.45×10^5). ^{1}H-NMR ($CDCl_3$; 400 MHz): δ 9.76, 9.55 and 8.56 (all s, 1H, meso-H); 7.76(s, 1H, ArH); 7.64 (d, J=6.8, 1H, ArH); 7.30 (d, J=8.0, 1H, ArH); 7.05 (t, J=8.2, 1H, ArH); 6.00 (q, J=6.9, 1H, 3^1-H); 5.28 (d, J=19.8, 1H, 13^2-CH_2); 5.13 (d, J=19.8, 1H, 13^2-CH_2); 4.70 (d, J=12.0, 1H, OCH_2Ar); 4.56 (dd, J=3.2,11.6, 1H, OCH_2Ar); 4.48-4.53 (m, 1H, 18-H); 4.30-4.33 (m, 1H, 17-H); 3.72 (q, J=8.0, 2H, 8-C<u>H</u>$_2$CH$_3$); 3.69, 3.61, 3.38 and 3.21 (all s, all 3H, for 17^3-CO_2CH_3 and 3 × ring CH_3); 2.66-2.74, 2.52-2.61 and 2.23-2.37 (m, 4H, 17^1-H and 17^2-H); 2.18 (dd, J=2.8, 6.4, 3H, 3^1-CH_3); 1.83 (d, J=8.0, 3H, 18-CH_3); 1.72 (t, J=7.6, 3H, 8-CH_2C<u>H</u>$_3$); 0.41 (brs, 1H, NH); -1.71 (brs, 1H, NH). HRMS for $C_{41}H_{43}N_4O_4I$: 783.2329 (Calculated, M + 1); Found: 783.2407. Anal. Calcd. For $C_{41}H_{43}N_4O_4I$: C, 62.91; H, 5.54; N, 7.16; I, 16.21. Found: C, 62.60; H, 5.59; N, 7.13; I16.45.

Synthesis of 3-{1'- (3-iodobenzyloxy)ethyl}purpurin-18-N-hexylimide methyl ester (4)

30% Hydrobromic acid (HBr) in acetic acid (2 mL) was added to purpurin-18-N-hexylimide methyl ester (100 mg, 0.15mmol) (23), and the reaction was stirred at room temperature for 2 h. After evaporating the acids under a high vacuum (0.1 mm Hg), excess of 3-iodobenzyl alcohol (0.45 mL, 20 fold excess), dry dichloromethane (5 mL) and anhydrous potassium carbonate (40 mg) were added. The reaction mixture was stirred under nitrogen atmosphere for 45 minutes. It was then diluted with dichloromethane (200 mL), washed with aqueous sodium bicarbonate solution (100ml) and then with water (2 × 200 mL). The dichloromethane layer was dried over anhydrous sodium sulphate, concentrated and treated with diazomethane. Evaporation of the solvent gave a syrupy residue, which was chromatographed over silica column using (1:4) Ethyl acetate: Hexanes as eluant to remove excess of 3-iodobenzylalcohol followed by (1:1) Ethyl acetate: Hexanes to yield 110 mg (81%) of the desired compound **4** which is sticky in nature. Analytical HPLC (Symmetry C18; 99/1: MeOH/H_2O): t_R = 38.71 min, >96%. UV-vis (MeOH): 701(4.31×10^4), 545 (2.15×10^4), 508 (7.32×10^3), 414 (1.31×10^5). ^{1}H-NMR ($CDCl_3$; 400 MHz): δ 9.72 (s, 1H, meso-H); 9.66 (s, 1H, meso-H); 8.58 (s, 1H, meso-H); 7.75 (s, 1H, ArH); 7.64 (d, J=9.2, 1H, ArH); 7.29 (d, J=7.2, 1H, ArH); 7.06 (dt, J=2.4, 7.4, 1H, ArH); 5.88 (q, J=6.2, 1H, 3^1-H); 5.41 (d, J= 8.8, 1H, 17-H); 4.68 (dd, J=2.6,12.6, 1H, OCH_2Ar); 4.55 (dd, J=3.2,12.0, 1H, OCH_2Ar); 4.45 (t, J=6.8, 2H, NC<u>H</u>$_2$(CH$_2$)$_4$CH$_3$); 4.37

(q, J=7.2, 1H, 18-H); 3.84 (s, 3H, 12-CH_3); 3.68 (q, J=7.6, 2H, 8-C$\underline{H}_2$$CH_3$); 3.56 (s, 3H, 17^2-CO_2CH_3); 3.31 (split s, 3H, 2-CH_3); 3.14 (s, 3H, 7-CH_3); 2.63-2.72 (m, 1H, 17^1-H); 2.38-2.48 (m, 1H, 17^2-H); 2.26-2.36 (m, 1H, 17^1-H); 2.12 (dd, J=2.2, 6.6, 3H, 3^1-CH_3); 1.95-2.05 (m, 3H, 17^2-H, and $NCH_2C\underline{H}_2(CH_2)_3CH_3$); 1.77 (d, J=7.2, 3H, 18-CH_3); 1.68 (t, J=7.6, 3H, 8-$CH_2C\underline{H}_3$); 1.56-1.61 (m, 2H, $N(CH_2)_2C\underline{H}_2(CH_2)_2CH_3$); 1.38-1.50 (m, 4H, $N(CH_2)_3(C\underline{H}_2)_2CH_3$); 0.95 (t, J=7.0, 3H, $N(CH_2)_5C\underline{H}_3$); -0.14 (brs, 1H, NH); -0.19 (brs, 1H, NH). HRMS for $C_{47}H_{54}N_5O_5I$: 896.3171 (Calculated, M + 1); Found: 896.3241.

Synthesis of 3-{1'- (Hexyloxy)ethyl}purpurin-18-N-(3-iodo)benzylimide methyl ester (5)

30% Hydrobromic acid (HBr) in acetic acid (2 mL) was added to purpurin-18-N-(3-iodo) benzylimide methyl ester (100 mg, 0.125 mmol) (23), and the reaction was stirred at room temperature for 2 h. After evaporating the acids under a high vacuum (0.1 mm Hg), an excess of n-hexanol (0.5 mL, 30 fold excess), dry dichloromethane (5 mL) and anhydrous potassium carbonate (25 mg) were added to the residue. The reaction mixture was stirred under nitrogen atmosphere for 45 minutes. It was then diluted with dichloromethane (200 mL), washed with aqueous sodium bicarbonate solution (100 mL) and then with water (2 × 200 mL). The dichloromethane layer was dried over anhydrous sodium sulphate, concentrated and treated with diazomethane. Evaporation of the solvent gave a syrupy residue, which was chromatographed over silica column using 1% acetone in dichloromethane as eluant to yield 95 mg (85%) of the desired compound **5**, which is sticky in nature. Analytical HPLC (Symmetry C18; 99/1: MeOH/H_2O): t_R = 48.97 min, >96%. UV-vis (MeOH): 700 (4.31×10^4), 545 (2.05×10^4), 508 (7.76×10^3), 414 (1.29×10^5). ^{1}H-NMR ($CDCl_3$; 400 MHz): δ 9.75 (splits, 1H, meso-H); 9.62 (s, 1H, meso-H); 8.53 (s, 1H, meso-H); 8.09 (s, 1H, ArH); 7.70 (d, J=7.6, 1H, ArH); 7.66 (d, J=8.0, 1H, ArH); 7.60 (d, J=7.6, 1H, ArH); 7.32 (d, J=8.4, 1H, ArH); 7.10 (t, J=7.8, 1H, ArH); 5.77 (q, J=6.8, 1H, 3^1-H); 5.61 (s, 2H, $NC\underline{H}_2Ar$); 5.37(d, J=8.4, 1H, 17-H); 4.35 (q, J=7.2, 1H, 18-H); 3.81 (s, 3H, 12-CH_3); 3.65 (m, 4H, 8-C$\underline{H}_2CH_3$, $OC\underline{H}_2(CH_2)_4CH_3$); 3.56 (s, 3H, 17^2-CO_2CH_3); 3.30 (s, 3H, 2-CH_3); 3.18 (s, 3H, 7-CH_3); 2.62-2.72 (m, 3H, $OCH_2C\underline{H}_2(CH_2)_3CH_3$ & 17^1-H); 2.30-2.45 (m, 2H, 17^2-H & 17^1-H); 2.05 (dd, J=2.4, 6.8, 3H, 3^1-CH_3); 1.95-2.02 (m, 1H, 17^2-H); 1.70-1.80 (m, 5H, 18-CH_3 & O $(CH_2)_2C\underline{H}_2(CH_2)_2CH_3$); 1.67 (t, J=8.0, 3H, 8-$CH_2C\underline{H}_3$); 1.23 (m, 4H, $O(CH_2)_3(C\underline{H}_2)_2CH_3$); 0.78 (m, 3H, $O(CH_2)_5C\underline{H}_3$); 0.04 (brs, 1H, NH); -0.07 (brs, 1H, NH). HRMS for $C_{47}H_{54}N_5O_5I$: 896.3171 (Calculated, M + 1); Found: 896.3241.

Synthesis of 3-{1'- (3-trimethylstannylbenzyloxy)ethyl}purpurin-18-N-hexylimide methyl ester (6)

To a solution of 3-{1'- (3-iodobenzyloxy)ethyl}purpurin-18-N-hexylimide methyl ester (**4**) (15 mg, 0.017 mmol) in dry THF(10mL) were added hexamethylditin (15μl, 0.072 mmol) and bis-(triphenylphosphine)palladium (II)dichloride (5 mg) and the reaction mixture was stirred at 60°C for 2 hours. The reaction mixture was rotavapoed to dryness and the crude product was purified over silica gel column using CH_2Cl_2 as eluant to yield 12 mg (77%) of title compound **6**. Analytical HPLC (Symmetry C18; 99/1: MeOH/H_2O): t_R = 48.19 min, >95%. ^{1}H-NMR ($CDCl_3$; 400 MHz): δ 9.73 (s, 1H, meso-H); 9.66 (s, 1H, meso-H); 8.56 (s, 1H, meso-H); 7.42(m, 2H, ArH); 7.34 (m, 2H, ArH); 5.90 (m, 1H, 3^1-H); 5.41 (dd, J= 2.6, 9.0, 1H, 17-H); 4.76 (dd, J=4.4,11.6, 1H, OCH_2Ar); 4.55 (dd, J=1.2,12.0, 1H, OCH_2Ar); 4.45(m, 2H, $NC\underline{H}_2(CH_2)_4CH_3$); 4.36 (q, J=7.3, 1H, 18-H); 3.85 (s, 3H, 12-CH_3); 3.68 (q, J=7.6, 2H, 8-C$\underline{H}_2CH_3$); 3.55 (s, 3H, 17^2-CO_2CH_3); 3.31 (split s, 3H, 2-CH_3); 3.11 (s, 3H, 7-CH_3); 2.63-2.72 (m, 1H, 17^1-H); 2.38-2.48 (m, 1H, 17^2-H); 2.26-2.36 (m, 1H, 17^1-H); 2.12 (dd, J=2.4, 6.8, 3H, 3^1-CH_3); 1.95-2.05 (m, 3H, 17^2-H & $NCH_2C\underline{H}_2(CH_2)_3CH_3$); 1.77 (d, J=7.2, 3H, 18-CH_3); 1.68(t, J=7.6, 3H, 8-$CH_2C\underline{H}_3$); 1.61(m, 2H, $N(CH_2)_2C\underline{H}_2(CH_2)_2CH_3$);1.38-1.50 (m, 4H, $N(CH_2)_3(C\underline{H}_2)_2CH_3$); 0.95 (t, J=7.2, 3H, $N(CH_2)_5C\underline{H}_3$); 0.18 (s, 9H, $Sn(CH_3)_3$); -0.09 (brs, 1H, NH); -0.16 (brs, 1H, NH).

Synthesis of 3-{1'- (hexyloxy)ethyl}purpurin-18-N-(3-trimethylstannyl)benzylimide methyl ester (7)

It was synthesized following the procedure described above for **6** from the respective compound 3-{1'- (hexyloxy)ethyl}purpurin-18-N-(3-iodo)benzylimide methyl ester (5). Yield: 75%. Analytical HPLC (Symmetry C18; 99/1: MeOH/H_2O): t_R = 53.13 min, >95%. ^{1}H-NMR($CDCl_3$; 400 MHz): δ 9.75 (splits, 1H, meso-H); 9.64 (s, 1H, meso-H); 8.53 (s, 1H, meso-H); 7.89 (s, 1H, ArH); 7.66 (d, J=8.0, 1H, ArH); 7.39 (d, J=7.2, 1H, ArH); 7.32 (m, H, ArH); 5.78 (q, J=6.6, 1H, 3^1-H); 5.68 (q, J=13.8, 2H, NCH_2Ar); 5.38 (d, J=8.0, 1H, 17-H); 4.35 (m, 1H, 18-H); 3.83 (s, 3H, 12-CH_3); 3.57-3.68 (m, 4H, 8-$C\underline{H}_2CH_3$, $OC\underline{H}_2(CH_2)_4CH_3$); 3.54 (s, 3H, 17^2-CO_2CH_3); 3.30 (s, 3H, 2-CH_3); 3.18 (s, 3H, 7-CH_3); 2.62-2.72 (m, 3H, $OCH_2C\underline{H}_2(CH_2)_3CH_3$ & 17^1-H); 2.30-2.45 (m, 2H, 17^2-H &17^1-H); 2.05 (dd, J=2.6, 6.6, 3H, 3^1-CH_3); 1.95-2.02 (m, 1H, 17^2-H); 1.73 (d,J=7.6,3H,18-CH_3); 1.67 (t, J=7.6, 3H, 8-$CH_2C\underline{H}_3$); 1.25 (m, 6H, $O(CH_2)_2(C\underline{H}_2)_3CH_3$); 0.78 (m, 3H, $O(CH_2)_5C\underline{H}_3$); 0.27 (s, 9H, $Sn(CH_3)_3$); -0.01(brs, 1H, NH); -0.13 (brs, 1H, NH).

Synthesis of 3-{1'- (methoxy)ethyl}purpurin-18-N-(3-iodo)benzylimide methyl ester (10)

It was prepared by following the method described for compound **5** except the intermediate bromo-derivative was reacted with methanol, instead of n-hexanol. Pure product was obtained by column chromatography over silica column using 1% acetone in dichloromethane as eluant. Analytical HPLC (Symmetry C18; 99/1: MeOH/H_2O): t_R = 31.42 min, >98%. UV-vis (CH_2Cl_2): 700 (4.31×10^4), 545 (2.12×10^4), 414 (1.29×10^5). ^{1}H-NMR($CDCl_3$; 400 MHz): δ 9.66 (s, 1H, meso-H); 9.64 (s, 1H, meso-H); 8.54 (s, 1H, meso-H); 8.08 (s, 1H, ArH); 7.70 (d, J=8.0, 1H, ArH); 7.60 (d, J=8.0, 1H, ArH); 7.10 (t, J=8.0, 1H, ArH); 5.73 (q, J=6.9, 1H, 3^1-H); 5.63 (s, 2H, $NC\underline{H}_2Ar$); 5.38 (dd, J=1.6, 8.4, 1H, 17-H); 4.35 (q, J=7.2, 1H, 18-H); 3.84 (s, 3H, 12-CH_3); 3.67 (q, J=7.4, 2H, 8-$C\underline{H}_2CH_3$); 3.56 (s, 3H, 17^2-CO_2CH_3); 3.54 (d, J=2.8, 3H, OCH_3); 3.32 (s, 3H, 2-CH_3); 3.19 (s, 3H, 7-CH_3); 2.62-2.72 (m, 1H, 17^1-H); 2.30-2.45 (m, 2H, 17^2-H & 17^1-H); 2.06 (dd, J=2.2, 6.6, 3H, 3^2-CH_3); 1.92-2.02 (m, 1H, 17^2-H); 1.76 (d, J=6.0, 3H, 18-CH_3); 1.68 (t, J=7.6, 3H, 8-$CH_2C\underline{H}_3$); 0.03 (brs, 1H, NH); -0.07 (brs, 1H, NH). HRMS for $C_{42}H_{44}N_5O_5I$: 826.2387 (Calculated, M + 1); Found: 826.2470.

Synthesis of 3-{1'- (methoxy)ethyl}purpurin-18-N-(3-trimethylstannyl)benzylimide methyl ester (11)

The title compound was synthesized following the procedure described above for compound **7** from the respective compound 3-{1'-(methoxy)ethyl}purpurin-18-N-(3-iodo)benzylimide methyl ester (10). Yield: 80%. Analytical HPLC (Symmetry C18; 99/1: MeOH/H_2O): t_R = 35.79 min, >98%. ^{1}H-NMR ($CDCl_3$; 400 MHz): δ 9.68 (s, 1H, meso-H); 9.65 (s, 1H, meso-H); 8.56 (s, 1H, meso-H); 7.90 (s, 1H, ArH); 7.68 (d, J=7.6, 1H, ArH); 7.40 (d, J=6.8, 1H, ArH); 7.34 (t, J=7.2, 1H, ArH); 5.60-5.80 (m, 3H, 3^1-H and $NC\underline{H}_2Ar$); 5.38 (dd, J=2.0, 6.8, 1H, 17-H); 4.36 (q, J=7.2, 1H, 18-H); 3.84 (s, 3H, 12-CH_3); 3.67 (q, J=7.4, 2H, 8-$C\underline{H}_2CH_3$); 3.56 (s, 3H, 17^2-CO_2CH_3); 3.55 (d, J=2.8, 3H, OCH_3); 3.33 (s, 3H, 2-CH_3); 3.20(s, 3H, 7-CH_3); 2.62-2.72 (m, 1H, 17^1-H); 2.30-2.50 (m, 2H, 17^2-H & 17^1-H); 2.08 (dd, J=2.2, 6.6, 3H, 3^2-CH_3); 1.92-2.02 (m, 1H, 17^2-H); 1.76 (d, J=7.2, 3H, 18-CH_3); 1.68 (t, J=7.8, 3H, 8-$CH_2C\underline{H}_3$); 0.28 (s, 9H, $Sn(CH_3)_3$); -0.03 (brs, 1H, NH); -0.12(brs, 1H, NH).

Radioactive Labeling—^{124}I-analogs of **4, 5** and **10** were prepared from the corresponding trimethylstannyl analogs **6, 7** and **11** respectively by following the procedure as described below for ^{124}I analog of compound **4**.

Synthesis of ^{124}I- labeled analog of 3-{1'- (3-iodobenzyloxy)ethyl}purpurin-18-N-hexylimide methyl ester (4)

The trimethyltin analog **6** (50 μg) was dissolved in 50 μl of 5% acetic acid in methanol. 100 μl of 5% acetic acid in methanol was added to $Na^{124}I$ in 10 μl of 0.1N NaOH. The two solutions were mixed and an IODOGEN® bead (Pierce Biotechnology, Inc., Rockford, IL 61106) was added. The reaction mixture was incubated at room temperature for 15 minutes, iodobead was removed and the reaction mixture was injected on HPLC column (Symmetry C18 5μ, 150 × 4.6mm), which was eluted with an isocratic 99/1: MeOH/H_2O at a flow rate of 1 ml/min.The UV detector was set at 254nm wavelength. The labeled product (**4**) eluted at 46.7 min was collected and the solvent was evaporated to dryness under stream of N_2 at 60°C. The product was formulated in saline containing 10% ethanol for *in vivo* experiments. RadioTLC confirmed the radiochemical purity (>95%) of the product. A standard curve was generated between peak area versus mass by injecting known mass of carrier **4** onto the column. The mass associated with the labeled product was calculated by relating the peak area of UV absorbance peak of **4** in the labeled product to the standard curve. The specific activity was obtained by dividing the activity of the labeled product collected by the calculated mass in micromoles. Specific activity of radio labeled product was >1 Ci/μmol. The radiochemical yield was found to be 40%.

PET Imaging—Mice were imaged in the micropet FOCUS 120®, a dedicated 3D small-animal PET scanner (Concorde Microsystems Incorporated) at State University of New York at Buffalo (south campus) under the Institutional Animal Care and use Committee (IACUC) guidelines. The C3H mice were subcutaneously injected with 3×10^5 RIF cells in 30 μl complete α- MEM (into the axilla) and tumors were grown until they reached 4-5 mm in diameter (approximately 5 days). All tumored C_3H mice were injected via the tail vein 50-200 μCi of **1, 8, 9** and **12**. After 24, 48, 72 and 96 h post injection the mice were anesthetized by inhalation of isoflurane/oxygen, placed head first prone for imaging and the acquisition time was set for 30 minutes. Radioiodine uptake by thyroid or stomach was not blocked.

Biodistribution studies—All studies were performed as per IACUC guidelines. The mice were injected with 50-200 μCi of **1, 8, 9** and **12** via tail vein and 3 or 4 mice each at 24, 48, 72 and 96 h time interval were sacrificed, and body organs (tumor, heart, liver, spleen, kidney, lung, muscle etc.) removed immediately. After weighing, the amount of radioactivity in the tumor (50-150 mg), body organs and blood was measured by a gamma well counter. Radioactivity uptake was calculated as the percentage of the injected dose per gram of the tissue (%ID/g). Statistical analyses and data (%ID/g vs. time point) were plotted using Microsoft Excel.

In vitro photosensitizing efficacy—The photosensitizing activity of **4, 5** & **10** was determined in the RIF tumor cell line. The RIF tumor cells were grown in α-MEM with 10% fetal calf serum, L-glutamine, penicillin, streptomycin and neomycin. Cells were maintained in 5% CO_2, 95% air and 100% humidity. For determining the PDT efficacy, these cells were plated in 96-well plates at a density of 5×10^3 cells well in complete media. After an overnight incubation at 37°C, the photosensitizers were added at variable concentrations and incubated at 37°C for 24 h in the dark. Prior to light treatment the cells were replaced with drug-free complete media. Cells were then illuminated with an argon-pumped dye laser set at 700 nm at a dose rate of 3.2 mW/cm^2 for 0-6 Joules/cm^2. After PDT, the cells were incubated for 48 h at 37°C in the dark. Following the 48 h incubation, 10 μl of 5.0mg/ml solution of 3-[4,5-dimethylthiazol-2-yl]-2,5-diphenyltetra-zoliumbromide (MTT) dissolved in PBS (Sigma, St. Louis, MO) was added to each well. After a 4 h incubation at 37°C the MTT and media were removed and 100 μl DMSO was added to solubilize the formazin crystals. The 96-well plate was read on a microtiter plate reader (Miles Inc. Titertek Multiscan Plus MK II) at an

absorbance of 560 nm. The results were plotted as percent survival of the corresponding dark (drug no light) control for each compound tested and each experiment was done with 4 replicate wells.

In vivo photosensitizing efficacy—The *in vivo* PDT experiments were performed in C3H mice when tumors grew to 4-5 mm in diameter (approx. day 5 post inoculation). The day before laser light treatment, all hair was removed from the inoculation site and the mice were injected intravenously with varying photosensitizer concentrations. At 24 h post-injection, the mice were restrained without anesthesia in Plexiglas holders and then treated with laser light from an argon-pumped dye laser tuned to emit drug-activating wavelengths as set by the monochromator (665 nm for 1, 705 nm for **4, 5** and **10**). The compounds were treated with light under similar treatment parameters under the fluence rate of 75 mW/cm^2 with a light dose of 135 J/cm^2. The mice were observed daily for signs of weight loss, necrotic scabbing, or tumor regrowth. If tumor growth appeared, the tumors were measured using two orthogonal measurements L and W (perpendicular to L) and the volumes were calculated using the formula $V = (L \times W^2)/2$ and recorded. Mice were considered cured if there was no sign of tumor regrowth by day 60 post-PDT treatment.

Results and Discussion

Chemistry

For the synthesis of desired compounds, methylpheophorbide-a, isolated from *Spirulina pacifica* was converted into purpurin-18 methyl ester by following the known methodology (44). For the preparation of 3-(1'-*m*-iodobenzyloxyethyl) analog **4**, it was first reacted with n-hexylamine, the intermediate amide derivative (isomeric mixture) so obtained on intramolecular cyclization under basic reaction conditions gave **2** in excellent yield. Further reaction of purpurinimide **2** with HBr/AcOH at room temperature produced the intermediate bromo- analog, which was dried under vacuum and immediately reacted with *m*-iodobenzyl alcohol to afford **4** as a mixture of methyl ester and the corresponding carboxylic acid, which on treating with diazomethane produced the methyl ester derivative **4** in >70% yield. For the synthesis of the related isomer **5**, purpurin-18 methyl ester was first refluxed with *m*-iodobenzyl amine and the intermediate **3** thus obtained on reacting with 1-hexanol by following the approach depicted in Scheme 1 gave the desired photosensitizer in modest yield. Compound **10** was synthesized from **3** following the methodology outlined for **5** and by replacing n-hexanol with methanol. For the preparation of the corresponding ^{124}I-analogs **8, 9** and **12**, the trimethylstannyl substituted analogs **6, 7** and **11** on electrophilic aromatic iodination with $Na^{124}I$ in the presence of iodogen beads afforded the ^{124}I-labeled purpurinimides **8, 9** and **12** with >95% radioactive specificity. The purity of final compounds (**4, 5** and **10**) was confirmed by NMR (experimental section) and HPLC analysis (See supporting Information).

Biological Studies

Comparative imaging and biodistribution of ^{124}I labeled purpurinimide isomers 8, 9 and 12—The PET imaging and biodistribution study of the radioactive purpurinimides **8** and were performed in C3H mice bearing RIF tumors. In a typical experiment, twelve tumored mice were injected with each compound (50-200μCi) and 3 mice/group were imaged at 24, 48, 72 and 96 h for 30 minutes with microPET (Siemens Preclinical Solutions, Knoxville, TN) and finally sacrificed after 96 h time point. Mice used in longitudinal imaging received higher activity (150-200uCi) compared to mice used in biodistribution alone (50-100 uCi).

For the biodistribution studies, selected organs [tumor, muscle, kidney, lungs, intestine (gut), stomach, spleen, heart and lung] were removed, weighed and measured in a gamma well counter. The tail was also taken into consideration in biodistribution studies to determine the

accuracy of injection. Interestingly, the two isomers showed a remarkable difference in imaging and biodistribution characteristics. The imaging and biodistribution data also correlated well with each other. Between the two isomers, isomer **8** (O-iodobenzyloxyethyl purpurinimide), had higher background (liver and spleen) and the tumor was not visualized. Although the tumor was also not significantly visualized with isomer **9** (N- (3-iodobenzyl purpurinimide), compared to compound **8**, the background images were not as high (Figure 2). If compared with the lead compound **1** (^{124}I-labeled), purpurinimide **9** also exhibited higher tumor uptake at 72 and 96 h PI, unfortunately higher background uptake negated tumor visualization (Figure 3). However in comparison of the ^{124}I- analog of pyropheophorbide **1**, both purpurinimide isomers **8** and **9** showed exceptionally high liver (32-fold and 8-fold respectively) and spleen uptake (85-fold and 3-fold respectively) at 24h PI. The significantly high uptake of purpurinimides **8** and **9** in liver and spleen resulted in non-visualization of the tumor and thus produced a poor contrast in whole body PET-imaging. Among isomers **8** and **9**, isomer **9** was selected for further modifications. The 1'-hexyloxyethyl group present at the top half of the molecule (position-3) was replaced with a methyl substituent. The resulting product **10**, with a reduced overall lipophilicity, was labeled with ^{124}I (compound **12**) and the PET imaging biodistribution data were performed in C3H mice bearing RIF tumors. The results obtained from the biodistribution studies suggest that the reduction in the overall lipophilicity of the molecule reduces the uptake of purpurinimide **12** in spleen and liver substantially and therefore enhances its tumor imaging capability at 96h post-injection. The biodistribution and whole-body PET imaging results obtained from compounds **1, 8, 9** and **12** suggest that for an efficient tumor imaging agent it is of utmost important to have a high uptake of the contrast agent in tumor with a faster clearance profile from other organs. This characteristic possibly explains the improved imaging capability of the lead compound **1** over other agents studied so far.

Comparative in vitro PDT efficacy—The *in vitro* phototosensitizing ability of the structural isomers **4** and **5** was compared at variable experimental conditions (MTT assay, see 'Experimental Section') in RIF cells. Both isomers were ineffective *in vitro* at lower light and drug doses. However as can be seen from Figure 4, at 24 h post-incubation and higher light dose (6.0 J/cm^2, drug concentration (1.0 μM and higher) isomer **5**, was more effective than the structural isomer **4**. Reducing the overall lipophilicity of **5**, by replacing the O-hexyl group at position-3 with an O-methyl group **10** produced enhanced efficacy over the isomers **4** and **5**.

In vivo PDT efficiency of pyropheophorbide-a 1 and purpurinimide isomers 4 & 5—The *in vivo* PDT efficacy of the isomers **4** and **5** was determined at three doses (1.0, 2.0 and 3.0μmol/kg) and was compared with the lead compound **1** in C3H mice bearing RIF tumors (5 mice/group). The tumors were exposed to light (λ_{max} = 705 nm for **4** and **5**; 665 nm for **1**, 135 J/cm^2, 75 mW/cm^2) at 24 h post injection. The tumor re-growth was measured daily. From the results summarized in Figure 5, it can be seen that compound **4** having the iodobenzyl group at the top half of the molecule, at a dose of 1.0 μmol/kg gave a good response (2/5 mice were tumor free on day 60). At the same dose the isomer **5** in which the iodobenzyl group is present at the lower half of the molecule did not gave any significant long-term tumor response. Under the same treatment parameters, compound **1** produced some tumor response, however it was more effective at a dose of 1.5 μmol/kg and 4/5 mice were tumor free on day 60. Among the isomers **4** and **5**, at higher doses (e.g. 2μmol/kg) compound **4** was toxic and all mice died within 24 h PDT treatment (Figure 5), whereas compound **5** did not show any significant activity. However at higher doses (2.5 and 3.0 μmol/kg) it was found to be quite effective

To investigate the effect of the overall lipophilicity in PDT efficacy, the hexyl ether group present at position-3 in **5** was replaced with a methyl ether substituent **10** and the biological efficacy of both the analogs was compared at doses of 1.0 and 2.5 mmol/kg., The tumors were treated with a laser light (λ_{max} = 705 nm, 135 J/cm^2, 75 mW/cm^2) at 24 h post-injection. From the results summarized in Figure 5 it can be seen that among the two analogs, the methyl ether

derivative **10** showed enhanced activity than the corresponding hexyl ether analog **5**, however, it was at least 1.5-fold less effective over the lead compound **1** derived from the methyl pyropheophorbide-a. For an accurate reflection of the actual therapeutic response, further studies with a larger group of mice under variable treatment parameters are currently in progress.

Conclusion

Our results suggest that the nature and the position of the substituents in purpurinimides makes a significant difference in the tumor uptake, which also reflects their imaging and PDT potential. Between the two structural isomers **4** and **5**, compound **5** containing an N- iodobenzyl group introduced at the bottom half of the purpurinimide showed improved imaging and phototherapeutic abilities than **4** where the iodobenzyl group was present at position-3 of the molecule. Decreasing the overall lipophilicity of compound **5** by substituting the hexyl ether with a methyl ether group (compound **10**) further improved its PET imaging ability and PDT efficacy. However, for establishing a correlation between the overall lipophilicity and tumor imaging potential, it is necessary to investigate a series of compounds within a particular system and these studies are currently in progress.

Supplementary Material

Refer to Web version on PubMed Central for supplementary material.

Acknowledgements

The financial support from the NIH (CA 114053, CA 127369 and CA 55791), the Oncologic Foundation of Buffalo, Roswell Park Alliance Foundation and the shared resources of the RPCI support grant (P30CA16056) is highly appreciated.

References

1. Massoud TF, Gambhir SS. Molecular imaging in living subjects: seeing fundamental biological processes in a new light. Gene Dev 2003;17:545–580. [PubMed: 12629038]
2. Verel I, Vissser GWM, van Dongen GA. The promise of immuno-PET in radioimmunotherapy. J Nucl Med 2005;46:164S–171S. [PubMed: 15653665]
3. Pentlow KS, Graham MC, Lambrecht RM, Daghighian F, Bacharach SL, Bendriem B, Finn RD, Jordan K, Kalaigian H, Karp JS, Robeson WR, Larson SM. Quantitative imaging of iodine-124 with PET. J Nucl Med 1996;37:1557–1562. [PubMed: 8790218]
4. González-Trotter DE, Manjeshwar RM, Doss M, Shaller C, Robinson MK, Tandon R, Adams GP, Adler LP. Quantitation of small-animal ^{124}I activity distributions using a clinical PET/CT scanner. J Nucl Med 2004;45:1237–1244. [PubMed: 15235072]
5. Sundaresan G, Yazaki PJ, Shively JE, Finn RD, Larson SM, Raubitschek AA, Williams LE, Chatziioannou AF, Gambhir SS, Wu AM. ^{124}I-Labeled engineered anti-CEA minibodies and diabodies allow high-contrast, antigen-specific small-animal PET imaging of xenografts in athymic mice. J Nucl Med 2003;44:1962–1969. [PubMed: 14660722]
6. Zanzonico P, O'Donoghue J, Chapman JD, Schneider R, Cai S, Larson S, Wen B, Chen Y, Finn R, Ruan S, Gerweck L, Humm J, Ling C. Iodine-124-labeled iodo-azomycin-galactoside imaging of tumor hypoxia in mice with serial microPET scanning. Eur J Nucl Med Mol Imag 2004;31:117–128.
7. Soghomonyan SA, Doubrovin M, Pike J, Luo X, Ittensohn M, Runyan JD, Balatoni J, Finn R, Tjuvajev JG, Blasberg R, Bermudes D. Positron emission tomography (PET) imaging of tumor-localized Salmonella expressing HSV1-TK. Cancer Gene Ther 2005;12:101–108. [PubMed: 15499377]
8. Robinson MK, Doss M, Shaller C, Narayanan D, Marks JD, Adler LP, González-Trotter DE, Adams GP. Quantitative immuno-positron emission tomography imaging of HER2-Positive tumor xenografts

with an Iodine-124 labeled anti-HER2 diabody. Cancer Res 2005;65:1471–1478. [PubMed: 15735035]

9. Dekker B, Keen H, Lyons S, Disley L, Hastings D, Reader A, Ottewell P, Watson A, Zweit J. MBP–annexin V radiolabeled directly with iodine-124 can be used to image apoptosis in vivo using PET. Nucl Med Biol 2005;32:241–252. [PubMed: 15820759]
10. Pinchuk AN, Rampy MA, Longino MA, Skinner RW, Gross MD, Weichert JP, Counsell RE. Synthesis and structure-activity relationship effects on the tumor avidity of aadioiodinated phospholipid ether analogues. J Med Chem 2006;49:2155–2165. [PubMed: 16570911]
11. Veach DR, Namavari M, Beresten T, Balatoni J, Minchenko M, Djaballah H, Finn RD, Clarkson B, Gelovani JG, Bornmann WG, Larson SM. Synthesis and in vitro examination of [^{124}I]-, [^{125}I]- and [^{131}I]-2-(4-iodophenylamino) pyrido[2,3-*d*]pyrimidin-7-one radiolabeled Abl kinase inhibitors. Nucl Med Biol 2005;32:313–321. [PubMed: 15878500]
12. Shaul M, Abourbeh G, Jacobson O, Rozen Y, Laky D, Levitzki A, Mishani E. Synthesis and in vitro examination of [^{124}I]-, [^{125}I]- and [^{131}I]-2-(4-iodophenylamino) pyrido[2,3-*d*]pyrimidin-7-one radiolabeled Abl kinase inhibitors. Bioorg Med Chem 2004;12:3421–3429. [PubMed: 15186828]
13. Schmidt MH, Reichert KW II, Ozker K, Meyer GA, Donohoe DL, Bajic DM, Whelan NT, Whelan HT. Preclinical evaluation of benzoporphyrin derivative combined with a light-emitting diode array for photodynamic therapy of brain tumors. Pediatr Neurosurg 1999;30:225–231. [PubMed: 10461068]
14. Whelan HT, Kras LH, Ozker K, Bajic D, Schmidt MH, Liu Y, Trembath LA, Uzum F, Meyer GA, Segura AD, Collier BD. Selective incorporation of In-111-labeled photofrin(tm) by glioma tissue in-vivo. J Neuro-oncol 1994;22:7–13.
15. Origitano TC, Karesh SM, Henkin RE, Halama JR, Reichman OH. Photodynamic therapy for intracranial neoplasms - investigations of photosensitizer uptake and distribution using In-111 photofrin-II single photon-emission computed-tomography scans in humans with intracranial neoplasms. Neurosurgery 1993;32:357–364. [PubMed: 8384325]
16. Nakajima S, Yamauchi H, Sakata I, Hayashi H, Yamazaki K, Maeda T, Kubo Y, Samejima N, Takemura T. In-111 labeled mn-metalloporphyrin for tumor imaging. Nucl Med Biol 1993;20:231–237. [PubMed: 8448578]
17. Subbarayan M, Shetty SJ, Srivastava TS, Noronha OP, Samuel AM, Mukhtar H. Water-soluble Tc-99m-labeled dendritic novel porphyrins tumor imaging and diagnosis. Biochem Biophys Res Commun 2001;281:32–36. [PubMed: 11178956]
18. Babbar AK, Singh AK, Goel HC, Chauhan UP, Sharma RK. Evaluation of Tc-99m-labeled photosan-3, a hematoporphyrin derivative, as a potential radiopharmaceutical for tumor scintigraphy. Nucl Med Biol 2000;27:587–592. [PubMed: 11056374]
19. Schuitmaker JJ, Feitsma RI, Journée-De Korver JG, Dubbelman TM, Pauwels EK. Tissue distribution of bacteriochlorin-a labeled with Tc-99m-pertechnetate in hamster greene melanoma. Int J Radiat Biol 1993;64:451–458. [PubMed: 7901307]
20. Lu XM, Fischman AJ, Stevens E, Lee TT, Strong L, Tompkins RG, Yarmush ML. Sn-chlorin e6 antibacterial immunoconjugates - an in vitro and in vivo analysis. J Immunol Methods 1992;156:85–99. [PubMed: 1431166]
21. Ma B, Li G, Kanter P, Lamonica D, Grossman Z, Pandey RK. N_2S_2-Tc-99m conjugates as tumor imaging agents: synthesis and biodistribution studies. J Porphyr Phthalocya 2003;1:500–507.
22. Westerman P, Glanzmann T, Andrejevic S, Braichotte DR, Forrer M, Wagnieres GA, Monnier P, van den Bergh H, Mach JP, Folli S. Long circulating half-life and high tumor selectivity of the photosensitizer meta-tetrahydroxyphenylchlorin conjugated to polyethylene glycol in nude mice grafted with a human colon carcinoma. Int J Cancer 1998;76:842–850. [PubMed: 9626351]
23. Vrouenraets MB, Visser GW, Stewart FA, Stigter M, Oppelaar H, Postmus PE, Snow GB, van Dongen GA. Development of meta-tetrahydroxyphenylchlorin-monoclonal antibody conjugates for photoimmunotherapy. Cancer Res 1999;59:1505–1513. [PubMed: 10197621]
24. Whelpton R, Michael-Titus AT, Jamdar RP, Abdillahi K, Grahn MF. Distribution and excretion of radiolabeled temoporfin in a murine tumor model. Photochem Photobiol 1996;63:885–891. [PubMed: 8992509]

25. Lawrence DS, Gibson SL, Nguyen ML, Whittemore KR, Whitten DG, Hilf R. Photosensitization and tissue distribution studies of the picket fence porphyrin, 3,1-tpro, a candidate for photodynamic therapy. Photochem Photobiol 1995;61:90–98. [PubMed: 7899498]
26. Wilson BC, VanLier JE. Radiolabeled photosensitizers for tumor imaging and photodynamic therapy. J Photochem Photobiol B 1989;3:459–463. [PubMed: 2504906]
27. Moore JV, Waller ML, Zhao S, Dodd NJ, Acton PD, Jeavons AP, Hastings DL. Feasibility of imaging photodynamic injury to tumours by high-resolution positron emission tomography. Eur J Nucl Med 1998;25:1248–1254. [PubMed: 9724373]
28. Lapointe D, Brasseur N, Cadorette J, La Madeleine C, Rodrigue S, van Lier JE, Lecomte R. High-Resolution PET imaging for in vivo monitoring of tumor response after photodynamic therapy in mice. J Nucl Med 1999;40:876–882. [PubMed: 10319764]
29. Berard V, Rousseau JA, Cadorette J, Hubert L, Bentourkia M, van Lier JE, Lecomte R. Dynamic imaging of transient metabolic processes by small-animal PET for the evaluation of photo sensitizers in photodynamic therapy of cancer. J Nucl Med 2006;47:1119–1126. [PubMed: 16818946]
30. Dong D, Dubeau L, Bading J, Nguyen K, Luna M, Yu H, Gazit-Bornstein G, Gordon EM, Gomer C, Hall FL, Gambhir SS, Lee AS. Spontaneous and controllable activation of suicide gene expression driven by the stress-inducible Grp78 promoter resulting in eradication of sizable human tumors. Hum Gene Ther 2004;15:553–561. [PubMed: 15212714]
31. Sugiyama M, Sakahara H, Sato K, Harada N, Fukumoto D, Kakiuchi T, Hirano T, Kohno E, Tsukada H. Evaluation of 3 ’-deoxy-3 ’-F-18-fluorothymidine for monitoring tumor response to radiotherapy and photodynamic therapy in mice. J Nucl Med 2004;45:1754–1758. [PubMed: 15471845]
32. Subbarayan M, Hafeli UO, Feyes DK, Unnithan J, Emancipator SN, Mukhtar H. A simplified method for preparation of Tc-99m-annexin V and its biologic evaluation for in vivo imaging of apoptosis after photodynamic therapy. J Nucl Med 2003;44:650–656. [PubMed: 12679412]
33. Henderson BW, Dougherty TJ. How does photodynamic therapy work? Photochem Photobiol 1992;55:145–157. [PubMed: 1603846]
34. Dougherty TJ, Gomer CJ, Henderson BW, Jori G, Kessel D, Korbelik M, Moan J, Peng Q. Photodynamic therapy. J Natl Cancer Inst 1998;90:889–905. [PubMed: 9637138]
35. Dolmans DE, Fukumura D, Jain RK. Photodynamic therapy for cancer. Nat Rev Cancer 2003;3:380–387. [PubMed: 12724736]
36. Pandey RK, Goswami LN, Chen Y, Gryshuk AL, Missert JR, Oseroff A, Dougherty TJ. Nature: A rich source for developing multifunctional agents. Tumor-imaging and photodynamic therapy. Lasers Surg Med 2006;38:445–467. [PubMed: 16788930]
37. Pandey SK, Chen Y, Zawada RH, Oseroff A, Pandey RK. Utility of tumor-avid photosensitizers in developing bifunctional agents for tumor imaging and/or phototherapy. Proceedings of SPIE, the International Society for Optical Engineering. Proceedings of SPIE 6139 2006:613905-1–613905-7.
38. Chen Y, Gryshuk AL, Achilefu S, Ohulchansky T, Potter W, Zhong T, Morgan J, Chance B, Prasad PN, Henderson BW, Oseroff A, Pandey RK. A novel approach to a bifunctional photosensitizer for tumor imaging and phototherapy. Bioconjugate Chem 2005;16:1264.
39. Li G, Slansky A, Dobhal MP, Goswami LN, Graham A, Chen Y, Kanter P, Alberico RA, Spernyak J, Morgan J, Mazurchuk R, Oseroff A, Grossman Z, Pandey RK. Chlorophyll-a analogues conjugated with aminobenzyl-DTPA as potential bifunctional agents for magnetic resonance imaging and photodynamic therapy. Bioconjugate Chem 2005;16:32–42.
40. Pandey SK, Gryshuk AL, Sajjad M, Zheng X, Chen Y, Abouzeid MM, Morgan J, Charamisinau I, Nabi HA, Oseroff A, Pandey RK. Multimodality agents for tumor imaging (PET, fluorescence) and photodynamic therapy. A possible “see and treat” approach. J Med Chem 2005;48:6286–6295. [PubMed: 16190755]
41. Pandey, SK.; Sajjad, M.; Chen, Y.; Batt, C.; Nabi, HA.; Oseroff, A.; Pandey, RK. Potential of chlorophyll based photosensitizer for detecting matastasis and photodynamic therapy. 54th Society of Nuclear Medicine Annual Meeting; Washington, DC, USA. June 2-6; 2007.
42. Gryshuk AL, Chen Y, Goswami LN, Pandey SK, Missert JR, Ohulchanskyy T, Potter W, Prasad PN, Oseroff A, Pandey RK. Structure-activity relationship among purpurinimides and bacteriopurpurinimides: Trifluoromethyl substituent enhanced the photosensitizing efficacy. J Med Chem 2007;50:1754–1767. [PubMed: 17371002]

43. Gryshuk AL, Graham A, Pandey SK, Potter WR, Missert JR, Oseroff A, Dougherty TJ, Pandey RK. A first comparative study of purpurinimide-based fluorinated vs. nonfluorinated photosensitizers for photodynamic therapy. Photochem Photobiol 2002;76:555–559. [PubMed: 12462653]

44. Zheng G, Potter WR, Camacho SH, Missert JR, Wang G, Bellnier DA, Henderson BW, Rodgers MA, Dougherty TJ, Pandey RK. Synthesis, photophysical properties, tumor uptake, and preliminary in vivo photosensitizing efficacy of a homologous series of 3-(1'-alkyloxy)ethyl-3-devinylpurpurin-18-N-alkylimides with variable lipophilicity. J Med Chem 2001;44:1540–1559. [PubMed: 11334564]

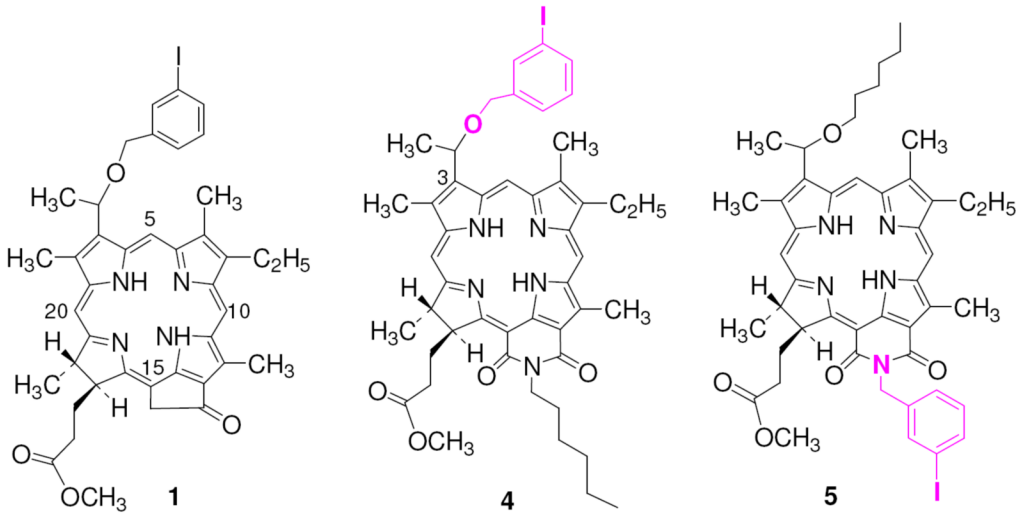

Figure 1.

Structures of 3-(1'-*m*-iodobenzyloxy) pyropheophorbide **1** and the iodobenzyl purpurinimides **4** and **5** (isomers)

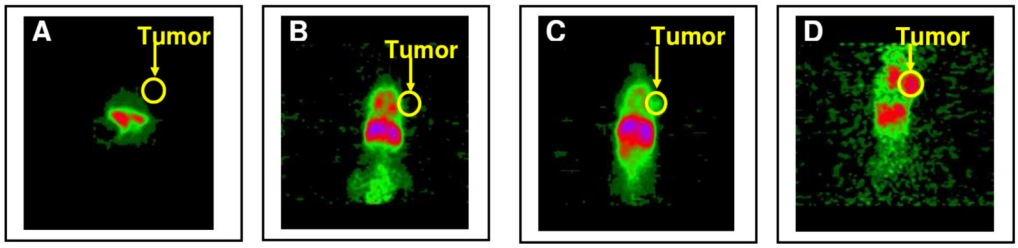

Figure 2.
Comparative microPET emission images (coronal view) of C3H mice with RIF tumors at 48 h PI of ^{124}I-124 labeled purpurinimides **9** (A), **9** (B), **12** (C) and (D) the lead compound **1**.

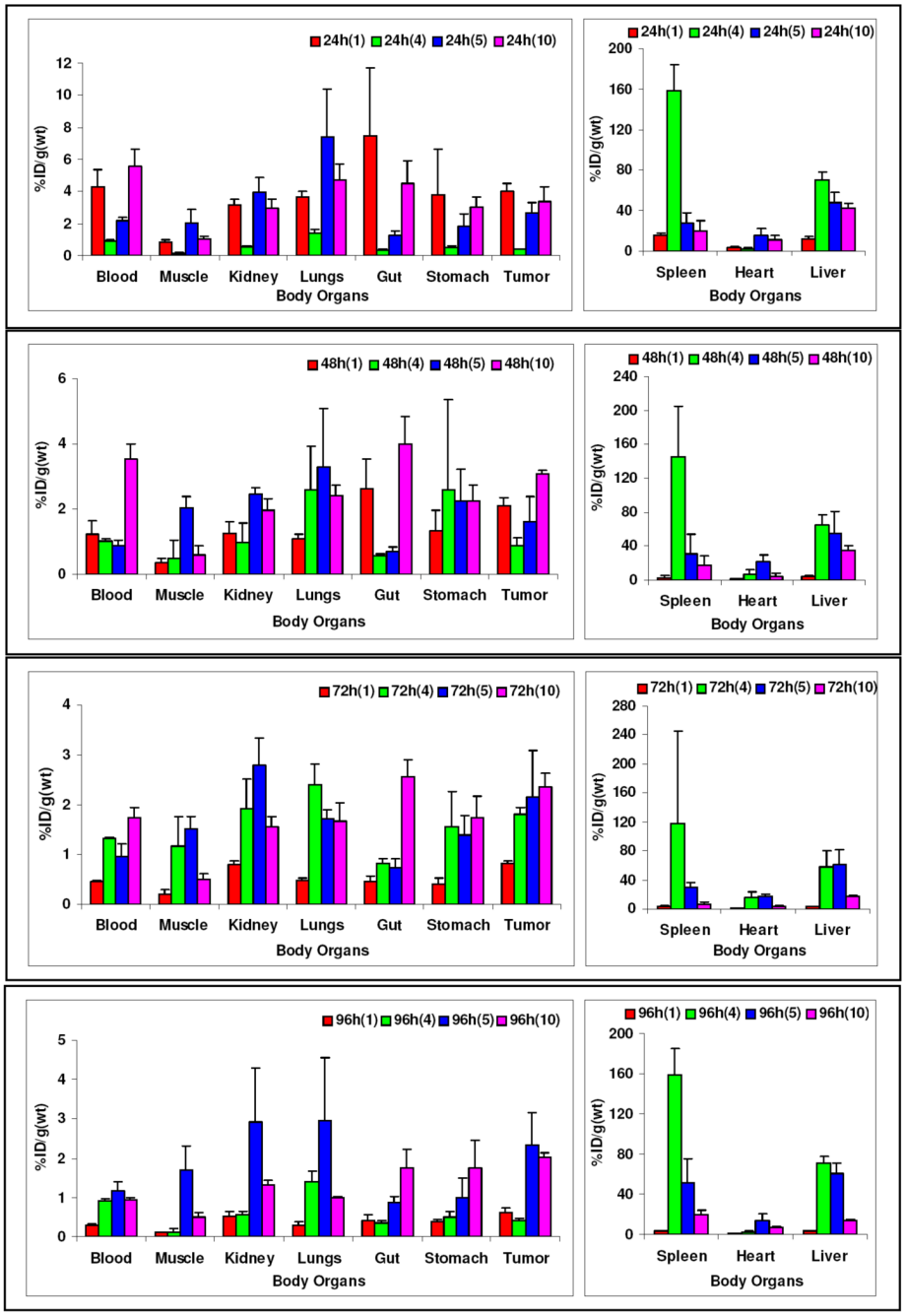

Figure 3.

Comparative biodistribution of (^{124}I-labeled) pyropheophorbide-**1** and the purpurinimides-**8, 9** and **12** at 24, 48, 72 and 96 h PI in C3H mice bearing RIF tumors (4 mice/time point). Note: Compounds **8, 9** and **12** are ^{124}l-labeled **4, 5** and **10** respectively.

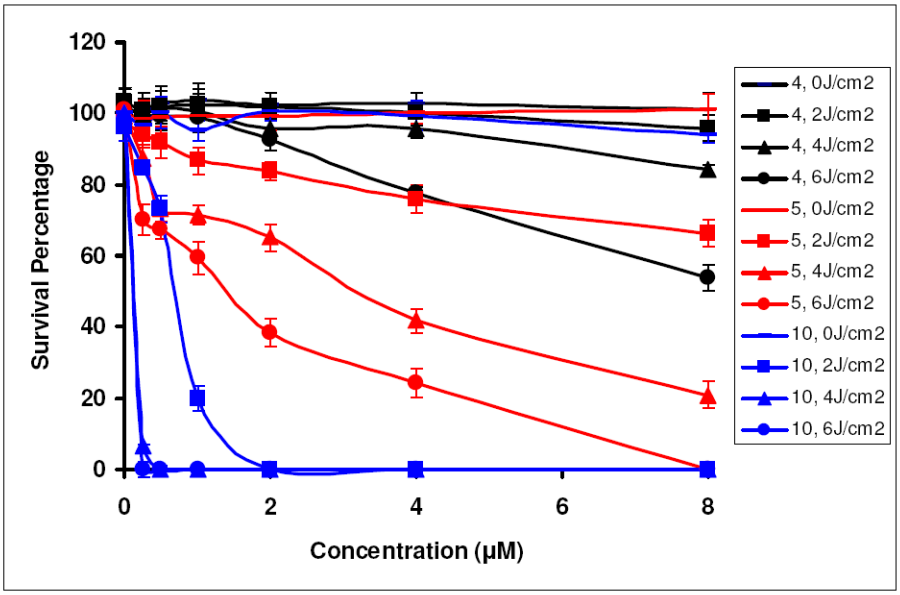

Figure 4.
Comparative *in vitro* photosensitizing activity of **4, 5** and **10** at variable drug concentrations and light doses in RIF tumor cells at 24 h post incubation

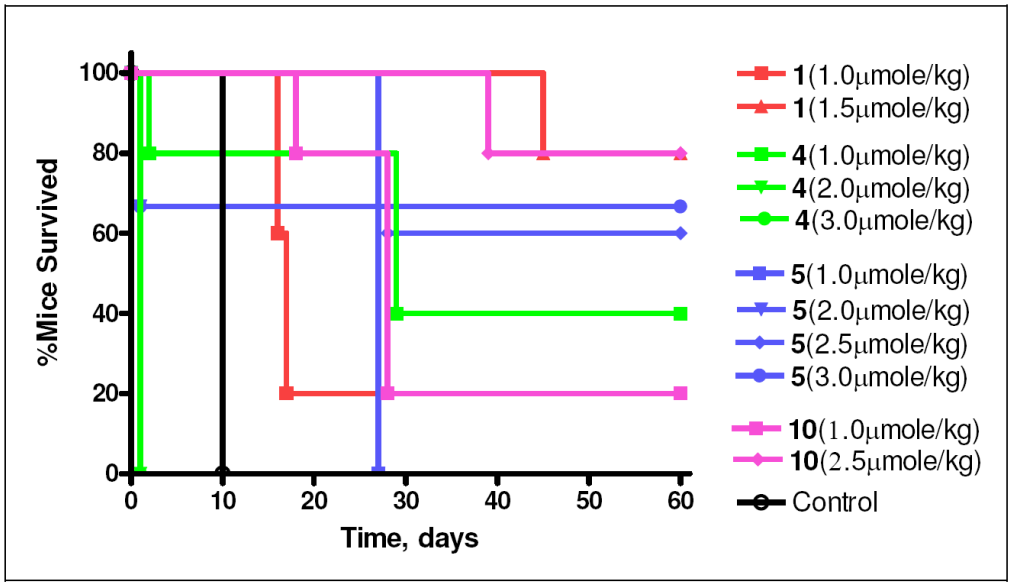

Figure 5.
Kaplan Meier plot for compounds **1, 4, 5** and **10** at various doses. C3H mice bearing RIF tumor (5mice/group) on the shoulder. Light dose: 135J/cm^2, 75 mW/cm^2 mice/group

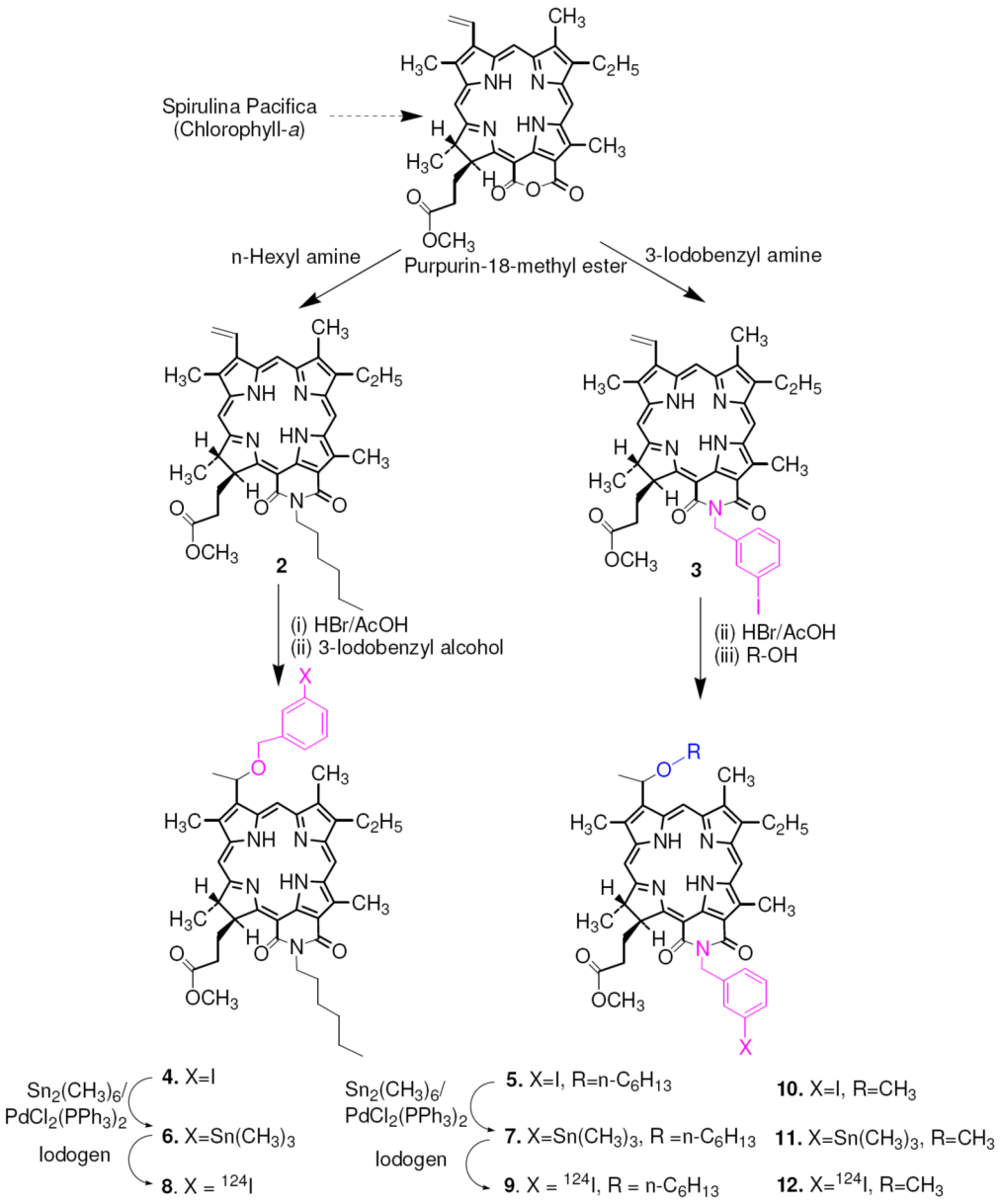

Scheme 1.
Syntheses of **4, 5** (structural isomers) & **10** and the corresponding ^{124}I-analogs **8, 9** and **12** respectively